The 2009 IEEE/RSJ International Conference on
Intelligent Robots and Systems
October 11-15, 2009 St. Louis, USA

Dynamic Analysis and Human Analogous Control of a Pipe Crawling Robot

Amir H.Heidari
Faculty of Engineering
University of Regina
Regina,SK,Canada
heydaria@uregina.ca

M.Mehrandezh
Faculty of Engineering
University of Regina
Regina, SK, Canada
Mehran.Mehrandezh@uregina.ca

R.Paranjape
Faculty of Engineering
University of Regina
Regina, SK, Canada
Raman.Paranjape@uregina.ca

H.Najjaran
School of Engineering
University of British Comulbia
Okanagon Campus, Canada
Homayoun.Najjaran@ubc.ca

***Abstract*— In this paper the design and development of a crawling robot for inspection of live water pipes are addressed. The mechanical design of the robot is described in detail. The governing dynamics equations of the robot moving against water flow as well as gravity in a straight pipe are also derived. Specifically, the hydrodynamic forces exerted on the robot when moving in a live pressurized pipe are taken into account. Two fuzzy-logic based control strategies are adopted. The first one is to maintain a constant translational speed in robot's motion when subjected to flow disturbances that are numerically modeled using step changes in flow velocity within a human-in-the-loop real-time simulation environment, and the second is to steer the real robot inside the pipe while following a numerically modeled time-varying velocity set point with no fluid present in the pipe. The controller parameters were tuned based on data obtained from a human-in-the-loop control system via an artificial neural network.**

I. INTRODUCTION

Well functioning water networks are essential to the sustainability of a community. Prevention and/or early detection of failures need a comprehensive assessment of pipe condition. Nondestructive/non-intrusive technologies for evaluating pipe condition are essential tools for the early detection. However, more research is required to adapt existing technologies to the unique circumstances of water mains that cannot be taken off service.

Various locomotion systems developed and cited in literature for in-pipe operations can be categorized into three main groups:

1) **Pipe Inspection Gauges (PIG) :** They are passive devices widely used for inspection of oil pipes and are designed so that sealing elements provide a positive interference with the pipe wall. Short inspection runs are costly and pipelines must be relatively clean for precise inspection [1],[2] .
2) **Floating systems/robots:** They are Underwater Autonomous Vehicles (UAV) and Remotely Operated Vehicles (ROV) used for data acquisition in sub-sea and deep-water missions. They have very limited applicability in confined environments such as pipes [3],[4].
3) **Mobile robots :** They are capable of carrying onboard sensors and testing devices through different pipe configurations [5]-[7]. Some popular variants of mobile robots for pipe inspection are *wheeled/tractor carriers* [8], *pipe crawlers* [9], *helical pipe rovers* [10],[11] and *walking robots* [12].

In this context, an underwater robotic vehicle was designed to carry pipe inspection instruments including Nondestructive Testing (NDT) sensors used for inspection of in-service water pipes of different materials. The robot can also provide real-time visual information about the interior surface of the pipe. The visual information and NDT data are synergistically used to make a more reliable decision about the condition of the pipe. The proposed system has the following features:

- It remains operational with pipeline in service.
- It has a very simple structure (i.e., the minimum number of moving parts/actuators).
- It is stable enough, throughout its motion, to maximize the performance of the inspection sensors.

Precise control of the robot's motion plays an important role in conducting effective assessment of the pipe's condition. Nonlinear friction, backlash in mechanical components and hydrodynamic forces exerted on the robot would require a nonlinear control design. An Adaptive Neuro-Fuzzy Inference System (ANFIS) [13] was adopted for this purpose where the parameters of the ANFIS were optimized based on experts' data obtained via a Human-In-The-Loop (HITL) real-time simulator.

Fuzzy control has achieved increasing attention among control engineers and in industrial systems specially where (1) no accurate model of the system under control is available and (2) one can take advantage of human experts available to provide linguistic rules for controlling the system. Mamdanis work [14] introduced this control strategy that Zedeh pioneered with his work in fuzzy sets [15]. He designed a fuzzy controller for control of a steam plant using the observed human expert efforts over a period of time controlling the plant.

The performance of fuzzy controllers depends on two significant issues, namely the soundness of knowledge acquisition techniques and availability of human experts. These two severely restrict the application domains of FLCs. ANFIS bypasses the former through tuning the FLC directly from a desired input-output data set.

This paper is organized as follows: in section II the details of the proposed design of the pipe crawler are addressed. In

section III the dynamics of the pipe crawler are detailed and its mathematical model is presented. Next in section IV the design of a PID controller and also a fuzzy logic controller for the servoing problem are explored and followed by that in section V where the simulation as well as experimental results are discussed. The conclusion and recommendations on further research are listed in section VI.

II. THE PROPOSED DESIGN OF THE PIPE CRAWLER

A. Design Factors

The principle objective put into practice in our design was to build a vehicle to serve as a highly stable platform capable of conducting precise sensing/scanning actions. The stability of the platform in terms of having smooth motion with regulated cruise speed is necessary for accommodating sensor readings at a high bandwidth. Precise positioning of the vehicle is particularly important for using precision probes to inspect and evaluate the condition of the inner surface of the pipes. The main design requirements of the robot are as follows:

1) The vehicle should be capable of completing inspection without decommissioning the pipeline.
2) The vehicle has to be pressure tolerant up to 20 atmospheres.
3) The sensor payload of the vehicle has to be flexible and user interchangeable.
4) Autonomy of the inspection process.
5) The robot should be designed in a way that it will not deteriorate the sanitation of the drinkable water when used in distribution water pipes.
6) The vehicle should be capable of traveling with any inclined pipe angle.
7) Finally, the vehicle should be able to stop and position itself at a specific location within the pipe using its onboard internal sensors, such as optical encoders.

B. The Proposed Vehicle Configuration

In our proposed system, we used low drag cylindrical shape modules as a platform for carrying inspection/navigation sensors and NDT devices. The symmetric shape of the robot can maintain a laminar boundary layer around its outer surface, thus the low-drag property enables the system to show superior stability against current in the pipe. Fig. (1) shows the robotic pipe crawler designed and studied here.

The robot consists of the following modules:

- *Nose Module :* This module accommodates a viewport for a digital still or a video camera.
- *Rechargable Battery Module :* It provides power for propulsion, system hardware, and sensors during mission.
- *Actuator, Control and Communication Module :* It accommodates the vehicle's actuator along with the control and communication electronics.

Further details on the design of the proposed robot can be found in [16].

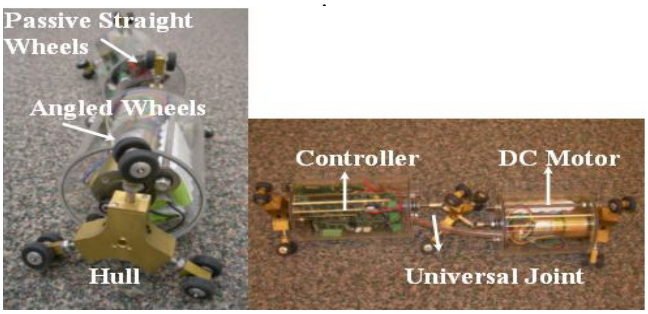

Fig. 1. The pipe inspection robot . (a) active and passive wheels. (b) side view of the robot.

Fig. (2) shows a simplified representation of the robot's driving mechanism. One should note that for simplicity we depicted two active wheels and also neglected the passive straight back wheels. As can be seen from Figs. (1) and (2), the driving wheels are positioned at a small angle with respect to the vertical plane which generates a screw type motion inside the pipe. The wheels are pushed against the inside wall of the pipe. The friction between the pipe's wall and the straight and unactuated wheels at the back of the robot prevents it from spinning.

This design provides simplicity and compactness while minimizing blockage of live pipes. Furthermore our proposed robot can negotiate pipes composed of straight and curved segments, thanks to the universal joints connecting the DC-motor to the hub.

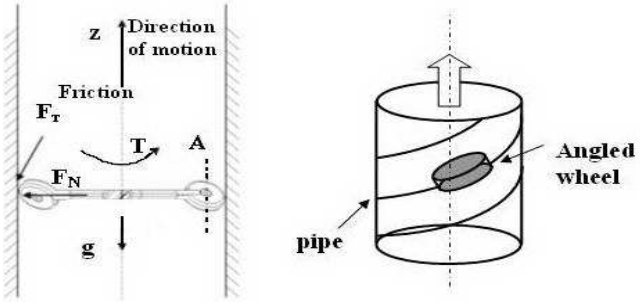

Fig. 2. The drive mechanism of the robot based on the principle of screw.

III. MOTION ANALYSIS

In this section the kinematics and kinetics of the proposed robot moving inside a vertical straight pipe are investigated. For simplicity, the dynamic equations are derived based on the following assumptions:

1. The angle of the driving wheels cannot change on fly;
2. The wheels apply a fixed amount of normal force to the pipe's wall preventing the slippage (i.e., no on-fly extension in arms is allowed).

The vehicle model and coordinate systems used in this study are shown in Fig. (3). It is assumed that one DC motor drives the hub and accordingly the wheels attached to the hull (or main body), as the prime actuator. From Fig. (3), frames i,

TABLE I

PHYSICAL PARAMETERS OF THE PIPE CRAWLER SYSTEM

Physical Properties of the System		
Symbol	Definition	Unit
m	Wheel Mass	Kg
M_h	Hull Mass	Kg
M_m	Motor Mass	Kg
r	Wheel Radius	m
A	Robot's Effective Cross Sectional Area	m^2
C_d	Drag Coefficient	$-$
μ	Fluid Dynamic Viscosity	$\frac{Kg}{m.s}$
ν	Downward Velocity of the Fluid	$\frac{m}{s}$
ρ	Fluid Density	$\frac{Kg}{m^3}$
K_f	Damping Constant	$N.m.s$
K_m	Toque Constant	$\frac{N.m}{A}$
K_b	Back EMF Constant	$\frac{N.m}{A}$
R	Motor Resistance	Ω
L	Motor Inductance	H
I_B	Hull Polar Moment of Inertia	$Kg.m^2$
I_{WZ},I_{WX}	Wheel Moment of Inertia	$Kg.m^2$
I_m	Motor Moment of Inertia	$Kg.m^2$
g	Gravitational Acceleration	$\frac{m}{s^2}$

B, and W represent the inertial fixed frame, the body frame attached to the main body of the robot, and the wheel frame attached to the wheel's center of rotation, respectively.

Physical parameters of the system in the presented dynamic

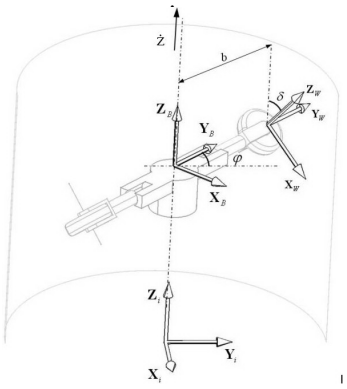

Fig. 3. The simplified model of the robot, with one pair of driving wheels, showing three reference frames.Passive wheels are not shown in this picture.

model of the robot and their definition are given in Table I.

A. Robot Kinematics

The infinitesimal translational displacement of the hull's COG, dz and the angular displacement of the wheel $d\theta$ can be expressed in terms of the infinitesimal angular displacement of the hull $d\phi$ by:

$$dz = (b+r)d\phi\tan(\delta) \tag{1}$$

$$d\theta = \left(\frac{b+r}{r\cos\delta}\right)d\phi; \qquad \delta \neq \frac{\pi}{2} \tag{2}$$

where δ is the wheel's inclination angle and b denotes the distance between the wheel's center of rotation and that for the hull.

B. Robot Dynamics

The dynamic equations of motion of the robotic vehicle can be derived using the standard Lagrangian approach. First we defined Lagrangian as:

$$L = T - V \tag{3}$$

where T and V denote the *kinetic energy* and the *potential energy* due to gravitational forces, respectively. The total kinetic energy of the robotic vehicle can be represented by:

$$T = T_{Motor} + T_{Hull} + \Gamma T_{AW} \tag{4}$$

whereT_{Motor}, T_{Hull} and T_{AW} denote kinetic energies of the motor, hull and the angled wheels, respectively, and Γ denotes the number of angled (active) wheels. In Eqn. (4), the kinetic energy of the passive straight wheels is disregarded. T_{Motor}, T_{Hull} and T_{AW} can be readily calculated as:

$$\begin{aligned} T_{Motor} &= \tfrac{1}{2}M_m\dot{z}^2 \\ T_{Hull} &= \tfrac{1}{2}M_h\dot{z}^2 + \tfrac{1}{2}I_B\dot{\phi}^2 \\ T_{AW} &= \left\{(mr^2 + I_{WZ})\left(\tfrac{bC_\delta}{b+r}\right)^2 + (mr^2 + I_{WX})S_\delta^2\right\}\tfrac{\dot{\theta}}{2} \end{aligned} \tag{5}$$

In Eqn. (5), S_δ and C_δ represent the short form of $\sin(\delta)$ and $\cos(\delta)$, respectively. Considering equations (1) and (5) the total kinetic energy of the system can be written as:

$$T = \frac{1}{2}\left\{\left((b+r)\frac{S_\delta}{C_\delta}\right)^2\alpha_M + \Gamma b^2\alpha_m + I_B\right\}\dot{\phi}^2 \tag{6}$$

where:

$$\begin{cases} \alpha_M = (M_m + M_h + \Gamma m + \Gamma\frac{I_{WX}}{r^2}) \\ \alpha_m = (m + \frac{I_{WZ}}{r^2}) \end{cases} \tag{7}$$

An infinitesimal change in the potential energy of the robot due to the gravity when moving in a vertical pipe can be calculated as:

$$dV = (M_m + N_h + \Gamma m)gdz \tag{8}$$

After substituting eqn. (1) in (8) one gets:

$$dV = (M_m + M_h + \Gamma m)(b+r)gd\phi\tan(\delta) \tag{9}$$

Considering the angle of rotation of the hull ϕ as the only generalized coordinate in the Lagrange formulation, one can write:

$$\frac{d}{dt}\left(\frac{\partial L}{\partial\dot{\phi}_i}\right) - \frac{\partial L}{\partial\phi} = Q \tag{10}$$

The generalized force Q applied on the robot moving inside the pipe can be given as:

$$Q = T_m - T_f - T_D \tag{11}$$

Where the right hand side of the above equation represents the non-potential generalized torques such as electromechanical torque generated by the motor, T_m, the resisting torques due to the friction between the wheels and their axles T_f, and the resisting torque due to hydrodynamic drag force posed on the system T_D all projected onto the generalized coordinate, ϕ.

Friction plays a significant role in creating the motion of the

robot. Insufficient friction at the point-of-contact between the wheels and the pipe's wall leads to wheel slippage. The slippage constraint of a wheel is expressed as (using Coulomb friction law):

$$F_T \leq \mu F_N \tag{12}$$

where μ denotes the friction coefficient, and F_N denotes the normal force applied on the internal surface of the pipe by the robot's wheels. Therefore, the resisting torque due to the internal friction can be obtained from the following equation:

$$T_f = \Gamma \mu b F_N + K_{f_1}\dot{\phi} + K_{f_2}\dot{\theta} \tag{13}$$

One should note that in Eqn. (13) :

1) $\Gamma \mu b F_N$ models the *coulomb friction* seen by the hub acting on the wheels.
2) $K_{f_1}\dot{\phi}$ and $K_{f_2}\dot{\theta}$ model the *viscous friction* on the hub and the wheels, respectively.

From Eqn. (2), the angular velocities of the hub and the wheels, namely $\dot{\phi}$ and $\dot{\theta}$ are related. Therefor one can write;

$$T_f = \Gamma \mu b F_N + K_f \dot{\phi} \tag{14}$$

where :

$$K_f = K_{f_1} + \frac{b+r}{rC_\delta} K_{f_2} \tag{15}$$

The hydrodynamic drag force induced by the flow on the robot, projected onto the generalized coordinate ϕ, can be expressed as follows:

$$T_D = bS_\delta \frac{\rho C_d A}{2}\Big((b+r)\dot{\phi}S_\delta + \nu\Big)^2 \tag{16}$$

where ρ, A, ν and C_d are as listed in Table I. One should note that in Eqn. (16):

1) The effect of the rotational motion of the robot on the drag coefficient is not considered, therefore, the drag coefficient is assumed to remain at constant as the robot moves.
2) Drag force on the wheels is negligible.

By substituting Eqns. (14) and (16) in Eqn. (11), the generalized force Q will be computed as:

$$Q = T_m - \Gamma \mu b F_N - K_f \dot{\phi} - bS_\delta \frac{\rho C_d A}{2}\Big((b+r)\dot{\theta}S_\delta + \nu\Big)^2 \tag{17}$$

By using Eqn. (17) and substituting T and V from Eqns. (6) and (9) into Eqn. (10), the following closed form solution in form of a nonlinear 2^{nd}-order differential equation for the wheels' motion (and correspondingly the robot's motion) can be obtained:

$$\ddot{\phi} = \frac{T_m - f(\dot{\phi}, \nu) - a_1}{a_2 + a_3 + I_B} \tag{18}$$

where:

$$\begin{cases} f(\dot{\phi}, \nu) = K_f \dot{\phi} + bS_\delta \frac{\rho C_d A}{2}\Big((b+r)\dot{\phi}S_\delta + \nu\Big)^2 \\ a_1 = \Gamma \mu b F_N + (M_m + M_h + \Gamma m)(b+r) g \tan(\delta) \\ a_2 = (M_m + M_h + \Gamma m + \Gamma \frac{I_{WX}}{r^2})\Big((b+r)\tan(\delta)\Big)^2 \\ a_3 = (m + \frac{I_{WZ}}{r^2})\Gamma b^2 \end{cases} \tag{19}$$

From Eqn. (18), one can realize that the motion of the robot can be controlled by changing parameters such as the wheel's inclination angle, δ the normal force exerted on the pipe's wall via the wheels, F_N, and the torque applied to the wheels' actuators, T_m. The only control input that can vary on fly in our design is the motor's torque, namely T_m. How to manipulate this torque in order to maintain a constant speed of motion when the robot is subjected to flow disturbances (i.e., variation in the flow speed, ν) will be discussed in section IV.

C. Motor Dynamics

The dynamics of a PMDC motor is represented by :

$$\frac{di_a}{dt} = -\frac{R}{L} i_a(t) - \frac{e_b}{L} + \frac{1}{L} v_{app}(t) \tag{20}$$

where $T_m = K_m i_a$ is the mechanical torque generated by the motor and $e_b(t) = K_b \dot{\phi}(t)$ is the back EMF of the motor. Here v_{app} is the input voltage (i.e., the control variable) and i_a denotes the armature current. In Eqn(20) it is assumed that the DC motor is not geared (i.e., direct drive).

IV. Controller Design

The primary objective of a controller is to provide appropriate inputs to a plant to obtain some desired output. In this research, the controller strives to reject hydrodynamic forces exerted on the robot due to flow disturbances while maintaining a constant speed for the robot. Two sets of disturbance models in form of step and also sinusoidal changes in flow velocity were generated randomly in a simulated environment. The controller tracks the response of the system to its user defined velocity set-point ($\dot{Z}_{set}$) and sends a correction command in terms of the input voltage provided to the DC motor actuators.
We compare the behavior of two controllers in this research: a conventional *Proportional plus Derivative plus Integral (PID)* controller and an ANFIS based *Fuzzy Logic Controller (FLC)* optimized through an artificial neural network where the ANFIS is trained based on data obtained from an operator through real-time HITL virtual reality simulator. More specifically parameters that define the membership functions on the inputs to the system and those that define the output of our system are tuned via ANFIS.

A. Fuzzy Logic Controller Design

ANFIS was the basis for the neuro-fuzzy controller that we developed. It consists of a multilayer neural network with each node performing a function such that the entire network is equivalent to a fuzzy system. ANFIS can learn fuzzy rules from input/output data, incorporate prior knowledge of fuzzy rules, fine tune the Membership Functions (MF) and act as a self-learning fuzzy controller by automatically generating the fuzzy rules needed. This capability of ANFIS was utilized to form a FL-based controller based on data obtained via HITL simulator.

1) Structure of the FLC: The rule-base of the proposed FLC contains rules of first order Takagi-Sugeno-Kang (TSK) type [17].

In our proposed FLC the two inputs to the controller are the error in linear velocity of the robot $e(t)$ and the rate of the change of the error $\dot{e}(t)$ as follows:

$$\begin{cases} e(t) &= \dot{Z}_{set} - \dot{z}(t); \\ \dot{e}(t) &= -\ddot{z}(t); \end{cases} \tag{21}$$

Here $\dot{z}(t)$ and $\ddot{z}(t)$ are the linear velocity and acceleration of the robot, repectively, and $\dot{Z}_{set}$ is the velocity set point. We used three sets of *product-of-two-sigmoidal* MF's on each input. These MF's are depicted in Fig. (4) and are represented by :

$$f(x; a_1, a_1, c_1, c_2) = \frac{1}{1 + e^{-a_1(x-c_1)}} \times \frac{1}{1 + e^{-a_2(x-c_2)}} \tag{22}$$

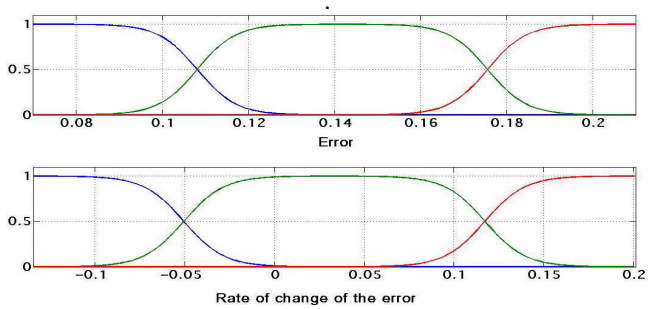

Fig. 4. Membership functions on the two inputs of the system : error and the rate of change in error before tuning.

2) Human-In-the-Loop Simulator: A real-time virtual reality HITL simulator was designed. Data acquired via this simulator were employed for training the ANFIS. The operator learns to control the velocity of the pipe crawler when subjected to flow disturbances via the Human-Machine Interface (HMI) designed for this purpose. Fig. (5) shows the closed-loop system modeled in the HITL simulator.

In order to acquire data from the controlled system and manipulate them in ANFIS for tuning our FLC, we used a HITL system where a human expert attempts to maintain the velocity of the robot at the desired set-point value $\dot{Z}_{set}$. In the proposed research we replace the "human operator" in Fig. (5) with a stand-alone FLC whose parameters are tuned using the data acquired from the human operator as depicted in Fig. (6). The disturbance on the system is simulated in form of step and sinusoidal changes in the flow velocity in the pipe.

3) Acquiring Real-Time Data: A joystick was used as the *haptic device* to control the voltage applied to the on-board DC motor actuator in both simulation environment and the experiments. The HMI used in this paper is shown in Fig. (7). In this figure, $\dot{z}(t)$ and $\dot{Z}_{set}$ are depicted on top with a solid and a dashed line, respectively. The randomly generated flow disturbance is shown at the bottom of the figure.

The operator can continuously monitor robot's motion in real-time to correct its course of motion by varying the voltage provided to the motor. The objective is to make $\dot{z}(t)$ closely follow $\dot{Z}_{set}$.

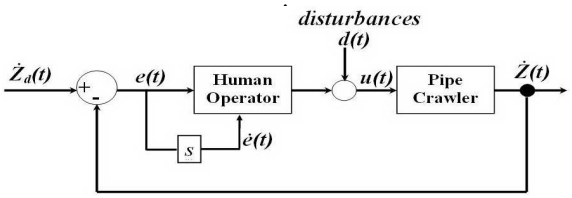

Fig. 5. Closed-loop system of the HITL simulator.

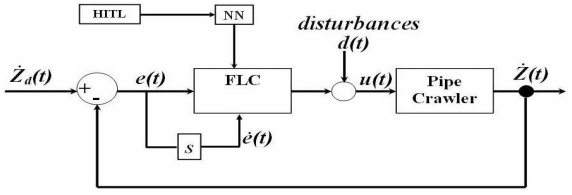

Fig. 6. FLC-based closed-loop system.

Following the above procedure, we asked our trainee to accomplish the control task in the presence of step flow disturbance as shown in Fig. (7). The trainees go through a few trials prior to real test. We chose the data-acquisition time to be $40s$, so that between each of the four jumps in the flow velocity is enough time for the human subject to bring the system back to its set-point. The MF's of the FLC after tuning them with ANFIS based on human data are shown in Fig. (8).

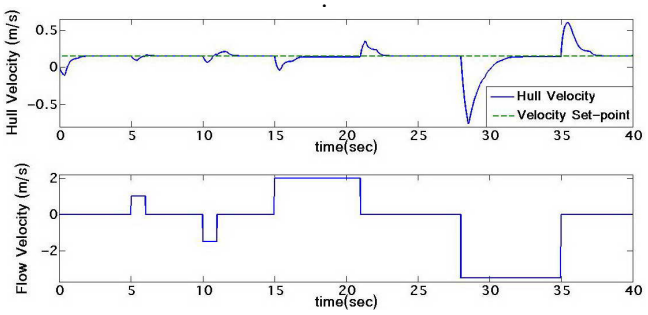

Fig. 7. A snapshot of the HMI used in this paper.

V. Simulation and Experimental Results

A. Simulation Results

MATLAB VR2008a together with *SIMULINK*, the *Fuzzy Logic Toolbox* and *WinCon V5.0* from Quanser [18] were used for real-time simulation of our proposed system. The control objective was to maintain a pre-set constant linear speed $\dot{Z}_{set}$ while moving the robot inside a vertical pipe in the presence of hydrodynamic forces due to flow.

1) External Disturbance Models: Two flow disturbance models were used in the simulation environment : (1) *step* changes and (2) *sinusoidal* changes in flow velocity as

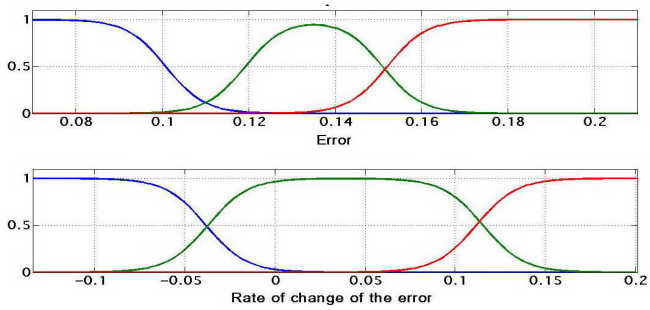

Fig. 8. Membership functions on the two inputs of the system : error and the rate of change in error after tuning.

depicted in Fig. (9) : A variety of simulations were conducted

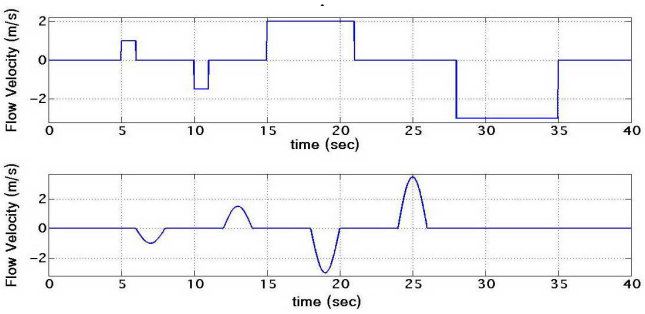

Fig. 9. Flow disturbance models used in simulation

based on the classical PID and also the stand-alone intelligent controller (FLC based on ANFIS), both of which were tested in a closed-loop system in the presence of the two aforementioned disturbance models and $\dot{Z}_{set} = 0.15\frac{m}{s}$

2) PID Controller: The tests were carried out with a classical PID controller of the form :

$$u(t) = K_p e(t) + K_d \frac{de}{dt} + K_I \int_0^t e(\tau)d\tau + u_0 \qquad (23)$$

The standard PID controller was designed in accordance with the Ziegler-Nichols tuning criteria [19]. The best value of gains were found to be $K_p = 20.4$, $K_i = 250$ and $K_d = 0.1285$ for proportional, integral and derivative gains, respectively. It is noteworthy that the term u_0 in Eqn. 23 is needed to compensate for the gravitational force applied to the robot (vertical pipe).

The response of the closed-loop system using a classical PID controller is shown in Fig. (10) and Fig. (11) .

3) Fuzzy Logic Controller: The FLC was further optimized using ANFIS based on the following procedure:

- *Training:* A human expert was trained to accomplish the control task within a Human-In-The-Loop real-time simulator in the presence of the flow disturbances explained above.
  One should note that for training purpose we used step changes in flow disturbance and $\dot{Z}_{set} = 0.15\frac{m}{s}$ as operating conditions. We will show through simulation that the FLC tuned based on ANFIS is capable of completing the servoing task under various operating conditions. Furthermore we will show that the FLC tuned based on ANFIS using human data acquired for this case (step flow disturbance) is capable of rejecting other forms of disturbance as well (e.g. sinusoidal).
- *Tuning FLC using ANFIS :* Next we used the above acquired data to tune the parameters of the FLC in ANFIS. The error tolerance in ANFIS was set at 10^{-6} and was reached after 97 epochs on average. The trend in the epochs and also the pertaining control surface is also depicted in Figs. (12) and (13) respectively.

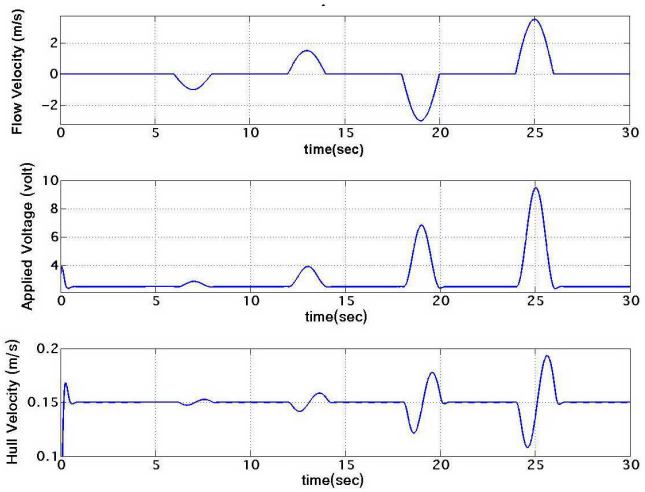

Fig. 10. Response of the closed-loop system with sinusoidal flow disturbance for $\dot{Z}_{set} = 0.15\frac{m}{s}$ using PID.

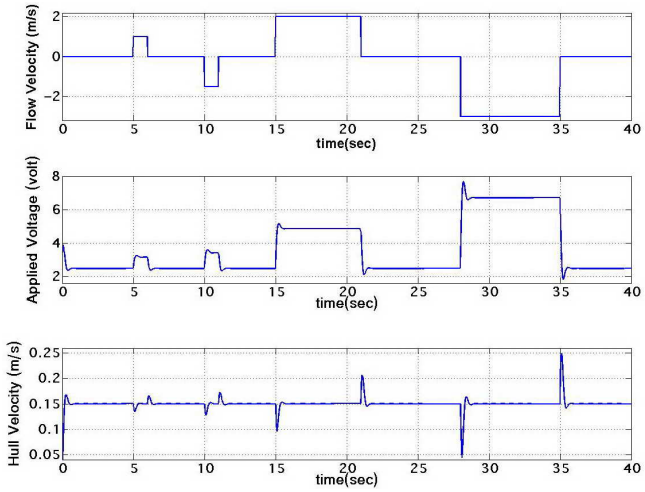

Fig. 11. Response of the closed-loop system with step flow disturbance for $\dot{Z}_{set} = 0.15\frac{m}{s}$ using PID.

The response of the closed-loop system using optimized FLC via ANFIS is depicted in Figs. (14) and (15). The above simulation results show that not only was the FLC capable of accomplishing the proposed servoing task, but it also posed the following three advantages over conventional PID controllers:

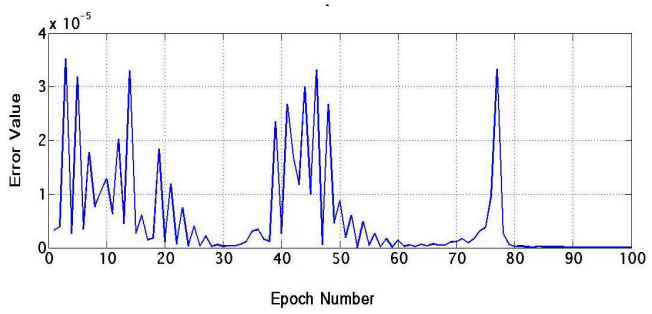

Fig. 12. Epoch evolution using ANFIS for sigmoidal membership function.

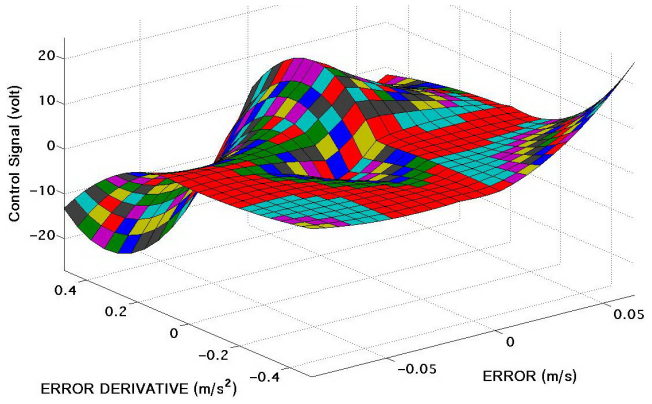

Fig. 13. Control Surface of the FLC using three sigmoidal MF's.

1) *Response Time* : the $(5-95)\%$ rise time, t_r of the closed-loop system was decreased by 283% (from $0.180s$ for PID to $0.047s$ for FLC).
2) *Energy Expenditure :* The control signal $u(t)$ used over the course of simulation was also decreased by using the proposed FLC. Table II summarizes the diffenerence in energy expenditure when the robot is subjected to different flow disturbances ($\dot{Z}_{set} = 0.15\frac{m}{s}$).

TABLE II

COMPARISON OF ENERGY EXPENDITURE (*volt.s*) BETWEEN FLC AND PID IN THE PRESENCE OF FLOW DISTURBANCE.

Flow Disturbance $\frac{m}{s}$	**FLC**	**PID**	**Improvement**
Sinusoidal	100.64	111.88	11.17%
Step	107.07	144.51	34.97%

3) *Actuator Saturation :* The control signal stays well below the saturation limit, i.e. $[-12, +12]volts$ when implementing the FLC in the closed-loop system. While in the PID controller, we reach the saturation limit at high amplitude external disturbances.

B. Experimental Results

1) Experimental Set Up: The real robotic pipe crawler was placed in a transparent PVC pipe of 6 inches in diameter for the experimentation. The controller's objective was to track the reference input in form of a time-varying linear velocity set-point. The trainee (using a joystick) attempts to maneuver the real robot so that it follows the velocity set-point visually represented in real time. Generally speaking, the same approach was followed as in simulation to tune the FLC parameters.

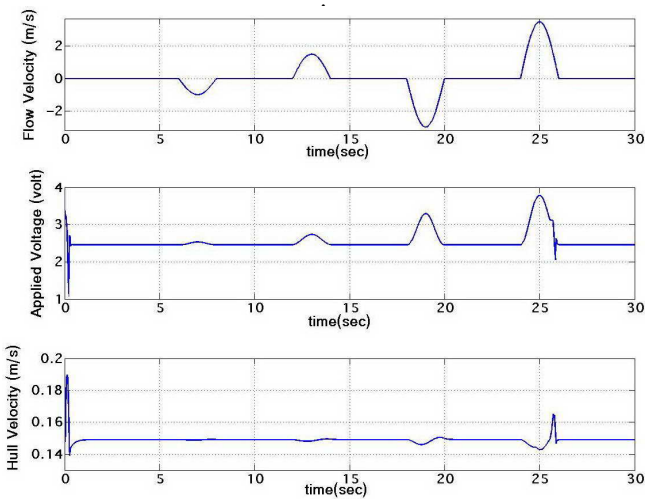

Fig. 14. Response of the closed-loop system with sinusoidal flow disturbance for $\dot{Z}_{set} = 0.15\frac{m}{s}$ using FLC.

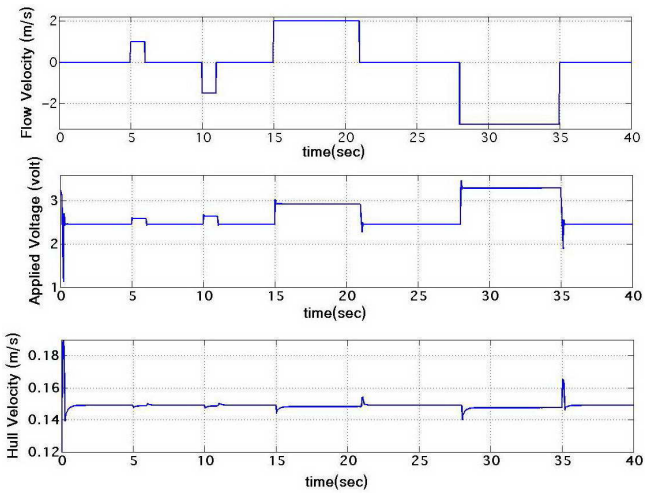

Fig. 15. Response of the closed-loop system with step flow disturbance for $\dot{Z}_{set} = 0.15\frac{m}{s}$ using FLC.

2) Data Acquisition for the Real System: The position and essentially the velocity of the robot inside the pipe were captured through the optical encoder mounted on the motor. These data, in turn, were fed into the processing unit (PC) through a Q4 DAQ board from Quanser [18].
Using a joystick as the haptic interface, the trainee, continuously receiving visual feedback on robot's motion on the monitor screen, applies a suitable voltage to the real system so that the linear velocity of the robot $\dot{z}(t)$ follows the desired trajectory of $\dot{Z}_{set}$.

3) Tuning FLC: The data of the final trial (after a few times of training) were fed into ANFIS to tune the FLC. One should note that the FLC utilized in the experimental set up holds the same structure (i.e. type and number of MF's)

used in simulation. After tuning the FLC through ANFIS, two experiments were conducted with a different $\dot{Z}_{set}$ for each, where the objective was to steer the robot along the pipe while $\dot{z}(t)$ follows the set point $\dot{Z}_{set}$ closely. The results are shown in Figs. (16) and (17) along with the control signal deployed. The human-analogous controller succeeded in carrying out the servoing task.

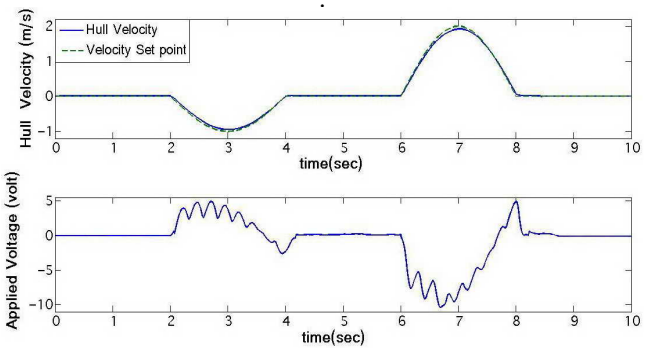

Fig. 16. Experimental results with sinusoidal reference trajectory of the velocity set point, $\dot{Z}_{set}$ using FLC.

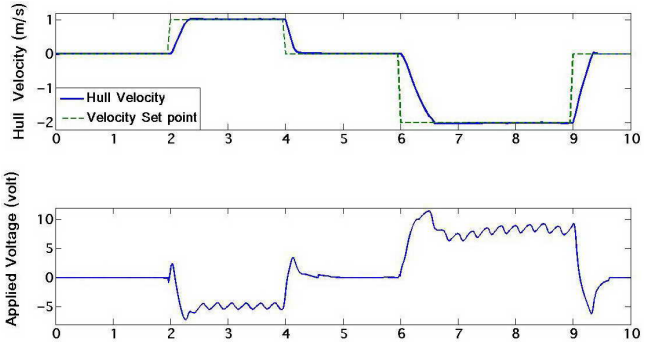

Fig. 17. Experimental results with step reference trajectory of the velocity set point, $\dot{Z}_{set}$ using FLC.

VI. CONCLUSIONS AND FUTURE WORKS

A. Conclusions

We addressed the design and development of a pipe crawler for inspection of water pipes along with the detailed derivation and analysis of its governing dynamic equations. Some beneficial aspects of the proposed design are autonomy in the inspection process, capability of doing the inspection without decommissioning the pipe line, and capability of traveling inside an inclined pipe. Also we implemented a new method for tuning the parameters of the FLC for pipe crawler's velocity regulation. The controller was designed based on TSK model and tuned using ANFIS based on data obtained from an operator via a real-time HITL virtual reality simulator. The controller was implemented in both simulation and experiment and it was shown that the proposed FLC outperforms a conventional PID controller.

B. Future Works

Future work has two folds: (1) developing a Hardware-In-the-Loop (HIL) simulation system to control the motion of the robot when located in an empty pipe (or duct) in a dry lab. A motorized flow simulator will be employed to simulate the effect of hydrodynamic forces exerted on the robot as it were moving inside a live pipe. The flow simulator and the robot will be connected via force sensors, (2) using a force/vision haptic interface for HITL control. The haptic device used in data acquisition was a regular joystick popular in video games. It's output limitation (in simulink) affects the precision of human action over the course of control task. With a specialized force/vision feedback control interface, the operator will be doing a more accurate job in controlling the robot's motion, and consequently the optimized human analogous FLC would yield better results.

REFERENCES

[1] Shiho, M., Horioka, K, et. al, Proposal for Environmental Observation System for Large Scale Gas Pipeline Networks using Unmanned Airship, *2nd International Symposium on Beamed Energy Propulsion Proceedings*, Issue 702, pp. 522-533, 2004.

[2] Nguyen, T. T., Yoo, H. R., et. al. Speed Control of PIG using Bypass Flow in Natural Gas Pipeline, *IEEE International Symposium on Industrail Electronics Proceedings*, Vol. 2, pp. 863-868, 2001.

[3] Gwyn Griffiths, Technology and applications of autonomous underwater vehicles, *Tylor & Francis Inc.*, 2003.

[4] F. Nickols, R. Bradbeer, and S.O. Harrold, An Ultrasonically Controlled Autonomous Model Submarine Operating in a Pipe Environment, *IEEE Conference on Mechatronics and Machine Vision Proceedings*, Toowoomba, Australia, September 1997.

[5] Koji, K. Underwater inspection robotAIRIS 21, *Journal of Nuclear Engineering and Design*, Vol. 188, Issue 3, pp. 367371, May 1999.

[6] Roh, S., and Choi, H. R., Differential-drive In-pipe Robot for Moving Inside Urban Gas Pipelines, *IEEE Transaction of Robotics*, Vol. 21, Issue 1, pp. 1-17, February 2005.

[7] Miwa Y., Satoh S., Hirose N., Remote-controlled Inspection Robot for Nuclear Facilities in Underwater Environment, *10th International Conference on Nuclear Engineering*, 2002.

[8] *http://www.inuktun.com/* (last visited, February 2009).

[9] Bradbeer, S. Harrold, Luk, B.L., Li, B., Yeung L.F., and Ho H.W. A Mobile Robot for Inspection of Liquid Filled Pipes, *Workshop on Service Automation and Robotics*, City University of Hong Kong, 2000.

[10] M. Horodinca, I. Doroftei, E. Mignon and A. Preumont, A simple architecture for in-pipe inspection robots, *International Colloquium on Mobile and Autonomous Systems*, June 25-26, 2002.

[11] *http://www.ulb.ac.be/scmero/robotics.html#pipe* (last visited, February 2009).

[12] *http://www.cityu.edu.hk/applied_research/electronics/FSE_EE_Robin Bradbeer_02.html* (last visited, February 2009).

[13] J.-S.R. Jang ,"ANFIS: Adaptive-Network-Based Fuzzy Inference Systems", *IEEE Transactions on Systems,Man and Cybernetics*, Vol. 23(03), pp.665-685, May 1993

[14] E.H. Mamdani,"Application of Fuzzy Algorithms for Control of Simple Dynamic Plant", *Proc. IEE 121* , Vol.12, pp.1585-1588,1974

[15] L.A. Zadeh, "Outline of a New Approach to the Analysis of Complex Systems and Decision Processes", *IEEE Transactions on Systems,Man and Cybernetics*, Vol. 3, pp.28-44, 1973

[16] Ratanasawanya, C., Binsirawanich, P., Yazdanjo, M., Mehrandezh, M., Poozesh, S., Paranjape, R., and Najjaran, H., Design and Development of a hardware-in-the-loop Simulation System for a Submersible Pipe Inspecting Robot, *Proc. Of the 2006 IEEE Canadian Conference on Electrical and Computer Engineering (CCECE06)*, pp.1526-1529, May 2006, Ottawa, Ontario, Canada.

[17] T.Takagi and M.Sugeno, "Fuzzy Identification of Systems and Its Applications to Modeling and Control", *IEEE Transactions on Systems,Man and Cybernetics*, Vol.15, Jan, 1985

[18] Quanser Consulting, *http://www.quanser.com* (last visited February 2009)

[19] J.G.Ziegler and N.B.Nichols, "Optimum settings for automatic controllers", *Trans. ASME*, Vol. 64, pp. 759-768, 1942